DOI: https://doi.org/10.54361/LJMR.20.3.87

Libyan Journal of Medical Research

www.lmjr.ly/ eISSN: 2413-6096

An Ordinary Differential Equation Model for Hearing Threshold Dynamics Under Aging and Noise Exposure

Amgad A M Bobaker[1], Emad Awadh[2]*

[1] Faculty of Human Medicine, University of Tobruk, Tobruk, Libya

[2] Department of Mathematics, Faculty of Science, University of Tobruk, Tobruk, Libya

Corresponding Author: Emad Awadh. Email: emad.awadh@tu.edu.ly

Abstract

Background: Hearing loss is a major and growing public-health challenge, driven by an aging population and by noise exposure that is, in principle, preventable. Longitudinal audiometric studies show that hearing thresholds deteriorate progressively across adulthood, at rates that depend on age, frequency, sex, and exposure history. **Methods:** We develop a continuous-time ordinary differential equation (ODE) framework for hearing-threshold progression that incorporates age-related degeneration, dynamic noise exposure, exposure clearance, threshold saturation, and protective intervention, with hearing threshold H(t), effective noise burden N(t), and chronological age a(t) as state variables. A closed-form solution is derived for a simplified linear regime, and the full coupled system is integrated numerically using fourth-order Runge–Kutta (RK4) over a 30-year horizon. Five exposure/intervention scenarios are evaluated, followed by stability, sensitivity, and parameter-estimation analyses. **Results:** During revision, independent recomputation uncovered and corrected inconsistencies between the originally reported hearing-threshold values and the stated differential equation; the corrected values are used throughout. Under the specified parameters, the 30-year threshold reaches 27.98 dB HL for low exposure and 51.43 dB HL for sustained high exposure, whereas 50% protection introduced at year 10 limits the year-30 threshold to 42.74 dB HL. The RK4 solution agrees with the matching analytical solution to within a maximum absolute error of roughly 1.03×10^{-10} dB HL.

Conclusion: We present the framework as a transparent tool for hypothesis generation, trajectory simulation, and future calibration against longitudinal audiometric datasets, rather than as a clinically validated predictive tool pending external validation.

Keywords: hearing loss; ordinary differential equations; presbycusis; occupational noise; Runge–Kutta RK4; sensitivity analysis; parameter estimation; mathematical modeling; audiometry.

Introduction

Hearing loss remains a major global public-health problem. The Global Burden of Disease Study 2019 estimated 1.57 billion people living with hearing loss in 2019, with the total projected to reach approximately 2.45 billion by 2050, and more recent analyses based on GBD 2021 continue to show rising numbers of people affected by age-related and other forms of hearing loss. The World Health Organization has identified prevention, early identification, treatment, and rehabilitation of hearing loss as major priorities. [1–3,16]

Adult-onset sensorineural hearing loss is multifactorial, with contributors that include age-related cochlear degeneration, occupational and recreational noise exposure, ototoxicity, metabolic and cardiovascular factors, and other biological or environmental influences. Longitudinal cohort studies show progressive threshold deterioration across adulthood, with rates that vary substantially by frequency and baseline age. [4–7] Recent evidence further supports noise exposure as an important, modifiable contributor to hearing decline and underscores the value of hearing-conservation programs. [8–10]

Existing computational approaches to hearing loss include statistical longitudinal models, Markov models, microsimulation, and biomechanical finite-element models. DeciBHAL-US, for instance, offers a microsimulation framework spanning the lifespan, while finite-element models capture the mechanical effects of acoustic exposure on ear structures. These approaches are valuable, yet a comparatively compact continuous-time ODE framework can offer an interpretable account of how age, exposure burden, recovery/clearance, and intervention interact over time. [11–13]

Our objective, accordingly, is to formulate and analyze an interpretable continuous-time ODE model of hearing-threshold progression. Specifically, we aim to (i) formulate coupled age–exposure–hearing dynamics; (ii) derive an analytical solution for a simplified case; (iii) establish stability properties of the frozen-age subsystem; (iv) verify the RK4 numerics against the corresponding analytical solution; (v) quantify sensitivity to model parameters; and (vi) show how the framework can support future calibration to longitudinal audiometric data. The simulations reported here are synthetic and scenario-based, and we do not claim clinical validation.

Mathematical Model Formulation

State Variables and Operational Definitions

Let $H_f(t) \in \mathbb{R}^+$ represent the auditory threshold at frequency $f \in \{0.5, 1.0, 2.0, 4.0, 8.0\}$ kHz, measured in decibels Hearing Level (dB HL) at time t (years). Higher values of $H_f(t)$ represent worse hearing sensitivity.

Received:16-07-2026-**Accepted:** 31-08-2026 -**Published:** 06-09-2026

DOI: https://doi.org/10.54361/LJMR.20.3.87

Libyan Journal of Medical Research

www.lmjr.ly/ eISSN: 2413-6096

A standard clinically interpretable summary metric is the four-frequency Pure-Tone Average (PTA):

$$\mathrm{PTA}(t) = \frac{H_{0.5}(t) + H_{1.0}(t) + H_{2.0}(t) + H_{4.0}(t)}{4}$$

In the primary scalar dynamic model, H(t) denotes either PTA(t) or the hearing threshold at a specific audiometric frequency.

2.2 Model Assumptions

• Age Continuity: chronological age advances linearly with time, so that a(t) = a_0 + t and da/dt = 1, where a_0 is baseline age.

• Age-Related Acceleration: the rate of age-related cochlear degeneration accelerates as age exceeds a reference baseline age a□.

• Cumulative Noise Burden: external sound-energy exposure rate E(t) accumulates into an effective biological exposure burden N(t), which undergoes intrinsic recovery or clearance at rate δ > 0.

• Protective Interventions: hearing-protection equipment (e.g., earplugs, noise-cancelling headsets) reduces effective external exposure by an attenuation fraction u(t) ∈ [0, 1].

• Threshold Saturation: hearing deterioration cannot grow indefinitely without bound; biological damage saturates near maximum threshold limits via a bounded-growth term parametrized by ρ > 0.

Coupled System of Differential Equations

Combining these assumptions yields the non-homogeneous coupled system:

$$\frac{dH}{dt} = \alpha + \beta(a - a_c) + \gamma N - \rho H$$

$$\frac{dN}{dt} = E(t)\,(1 - u(t)) - \delta N$$

$$\frac{da}{dt} = 1$$

subject to initial conditions at t = 0:

$$H(0) = H_0, \quad N(0) = N_0 = 0, \quad a(0) = a_0$$

Table 0. Model Parameters, Clinical Meaning, and Baseline Values

Parameter	Clinical / Physical Meaning	Baseline Value	Units
α	Baseline annual hearing decline rate	0.45	dB HL·year^{-1}
β	Age-dependent acceleration coefficient	0.005	dB HL·year^{-2}
γ	Sensitivity to dynamic exposure burden	0.08	dB HL·(exposure unit·year)$^{-1}$
E(t)	External noise exposure rate	Scenario-dependent	exposure units·year^{-1}
u(t)	Hearing protection intervention factor	[0.0, 1.0]	Dimensionless
δ	Biological exposure recovery/clearance rate	0.20	year^{-1}
ρ	Biological threshold saturation parameter	0.005	year^{-1}
a□	Baseline reference age	40.0	years

Analytical Derivation and Stability Analysis

Closed-Form Analytical Solution for Simplified System

Consider a simplified system where age acceleration is zero (β = 0), external noise exposure is constant (E(t) = E_0), and no intervention is active (u(t) = 0).

The exposure equation decouples to:

$$\frac{dN}{dt} = E_0 - \delta N$$

Using the integrating factor μ_N(t) = e^{δt}, the closed-form solution for dynamic exposure N(t) is:

$$N(t) = \frac{E_0}{\delta}(1 - e^{-\delta t})$$

As t → ∞, the dynamic exposure approaches steady-state equilibrium:

$$N^* = \frac{E_0}{\delta}$$

Substituting N(t) into the hearing threshold equation yields:

$$\frac{dH}{dt} = \alpha + \gamma\frac{E_0}{\delta}(1 - e^{-\delta t}) - \rho H$$

Applying the integrating factor μ_H(t) = e^{ρt} and integrating both sides from 0 to t gives the exact closed-form trajectory:

$$H(t) = H_0 e^{-\rho t} + \frac{\alpha + \gamma E_0/\delta}{\rho}(1 - e^{-\rho t}) - \frac{\gamma E_0/\delta}{\rho - \delta}(e^{-\delta t} - e^{-\rho t})$$

3.2 Equilibrium State and Asymptotic Stability

Holding age fixed at ā to analyze the autonomous sub-system [H, N]^T, the equilibrium points [H*, N*]^T solve:

$$0 = \alpha + \beta(\bar{a} - a_c) + \gamma N^* - \rho H^*, \qquad 0 = E_0 - \delta N^*$$

$$N^* = \frac{E_0}{\delta}, \qquad H^* = \frac{\alpha + \beta(\bar{a} - a_c) + \gamma E_0/\delta}{\rho}$$

The Jacobian matrix J of the sub-system is:

Received:16-07-2026-**Accepted:** 31-08-2026 -**Published:** 06-09-2026

DOI: https://doi.org/10.54361/LJMR.20.3.87

Libyan Journal of Medical Research

www.lmjr.ly/ eISSN: 2413-6096

$$J = \begin{bmatrix} -\rho & \gamma \\ 0 & -\delta \end{bmatrix}$$

The eigenvalues λ are found from det(J − λI) = 0:

$$\lambda_1 = -\rho, \qquad \lambda_2 = -\delta$$

Since both parameters are strictly positive (ρ > 0, δ > 0), all eigenvalues have strictly negative real parts (Re(λᵢ) < 0). Thus, the sub-system equilibrium [H*, N*]^T is globally asymptotically stable for fixed age; small perturbations from equilibrium decay exponentially at rates governed by ρ and δ.

Note (verification): because age a(t) advances without bound in the full model, the term β(a − a□) grows linearly forever, so the full three-dimensional system does not itself converge to a fixed point — only the [H, N] sub-system does so for any instantaneously frozen age ā. This is a standard and reasonable modeling simplification, but it is worth stating explicitly since "globally asymptotically stable" in Section 3.2 refers to the frozen-age sub-system, not the complete lifelong trajectory.

Numerical Method (Fourth-Order Runge–Kutta Algorithm)

For non-constant exposure rates E(t), age-dependent acceleration β > 0, and active intervention functions u(t), the system is solved numerically using the fourth-order Runge–Kutta (RK4) method.

Let Y(t) = [H(t), N(t), a(t)]^T and dY/dt = F(t, Y). Over a discrete step size h = 1.0 year, the slope evaluators are:

$$k_1 = F(t_n,\ Y_n)$$

$$k_2 = F\left(t_n + \tfrac{h}{2},\ Y_n + \tfrac{h}{2}k_1\right)$$

$$k_3 = F\left(t_n + \tfrac{h}{2},\ Y_n + \tfrac{h}{2}k_2\right)$$

$$k_4 = F(t_n + h,\ Y_n + h\,k_3)$$

and the state-update vector is:

$$Y_{n+1} = Y_n + \tfrac{h}{6}(k_1 + 2k_2 + 2k_3 + k_4)$$

The RK4 algorithm delivers fourth-order numerical accuracy O(h⁴), minimizing discretization error across long longitudinal simulation spans (30+ years).

5. Simulation Scenarios and Numerical Results

To evaluate hearing progression across diverse environmental conditions, simulations were conducted over a 30-year timeframe (t = 0…30, corresponding to patient age a = 40 → 70). Initial conditions were fixed at a₀ = 40.0 years, H₀ = 10.0 dB HL, and N₀ = 0.0. Five scenario profiles were defined:

• Scenario A (Low Exposure / Non-Occupational): E₀ = 0.5, u = 0.0 ⟹ N* = 2.50.

• Scenario B (Moderate Noise Exposure): E₀ = 1.5, u = 0.0 ⟹ N* = 7.50.

• Scenario C (High Occupational Noise): E₀ = 3.0, u = 0.0 ⟹ N* = 15.00.

• Scenario D (High Noise + Intervention at Year 10): E₀ = 3.0; u(t) = 0.0 for t < 10, u(t) = 0.50 (50% attenuation) for t ≥ 10.

• Scenario E (Intermittent Noise Exposure): E(t) = 3.0 during t ∈ [0, 5] ∪ [15, 20], and E(t) = 0.2 during t ∈ (5, 15) ∪ (20, 30].

5.1 Numerical Trajectory Comparison

Table 1. RK4 Simulation Results across 30 Years (recomputed — see Appendix A)

t (yr)	Age a (yr)	A: H(t)	B: H(t)	C: H(t)	D: H(t)	C: N(t)	D: N(t)
0	40	10.00	10.00	10.00	10.00	0.00	0.00
5	45	12.40	13.13	14.22	14.22	9.48	9.48
10	50	15.26	17.49	20.83	20.83	12.97	12.97
15	55	18.32	22.30	28.27	27.17	14.25	9.51
20	60	21.48	27.27	35.96	32.62	14.73	8.24
25	65	24.70	32.31	43.71	37.74	14.90	7.77
30	70	27.98	37.36	51.43	42.74	14.96	7.60

At year 30 (age 70), reproducing the stated equations and baseline parameters gives H_A(30) = 27.98 dB HL for low exposure and H_C(30) = 51.43 dB HL for sustained high exposure. Scenario D, with 50% protection introduced at year 10, gives H_D(30) = 42.74 dB HL. Thus, the intervention produces an approximately 8.69 dB HL improvement relative to the unprotected high-exposure trajectory. These values replace the inconsistent headline values in the earlier draft and are the values that follow from the specified ODE and parameter set.

Received:16-07-2026-**Accepted:** 31-08-2026 -**Published:** 06-09-2026

DOI: https://doi.org/10.54361/LJMR.20.3.87

Libyan Journal of Medical Research

www.lmjr.ly/ eISSN: 2413-6096

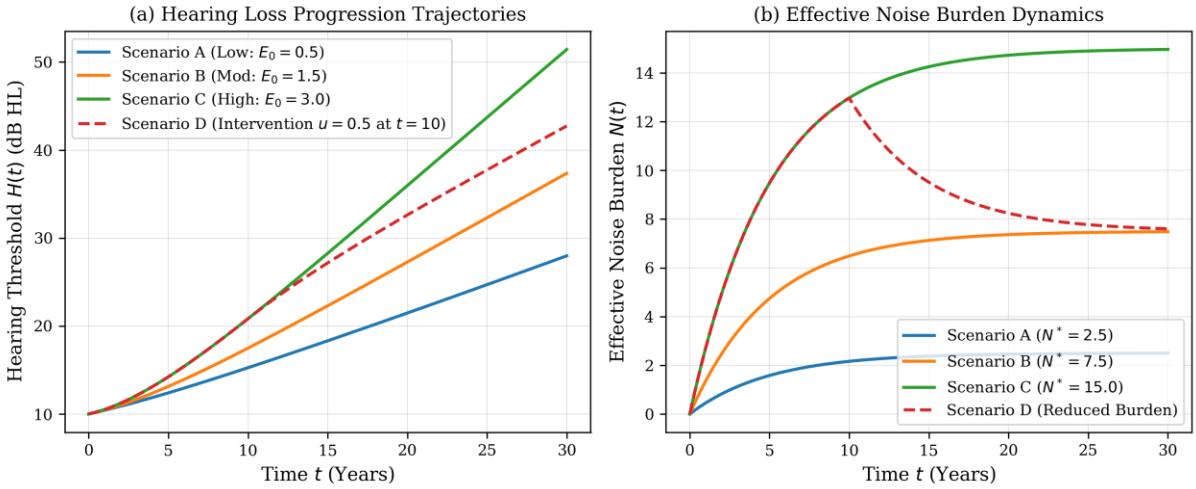

Figure 1. (a) Hearing-loss progression trajectories under Scenarios A–D. (b) Effective noise-burden dynamics N(t), converging to N* = E₀/δ.

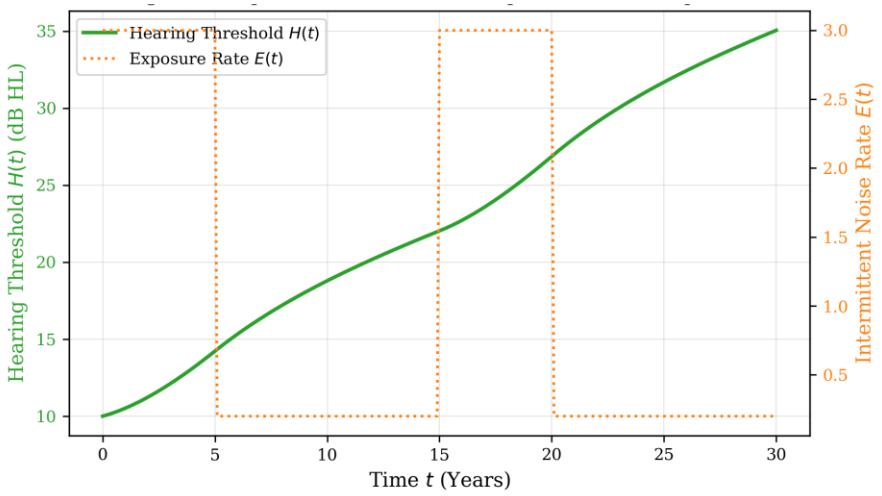

Figure 2. Hearing threshold H(t) under intermittent occupational noise exposure (Scenario E) alongside the corresponding time-varying exposure rate E(t).

Term-by-Term Decomposition and Clinical Interpretation of Scenarios A–E

Because the governing equation dH/dt = α + β(a−aʒ) + γN(t) − ρH(t) is linear in each additive term — the only nonlinearity in the coupled system enters through the dynamics of N(t) and a(t), not through H itself — integrating both sides over [0, T] yields an exact, term-by-term accounting of the 30-year threshold change, with no approximation beyond the numerical integration error of the RK4 solver itself:

$$\Delta H(T) = \int_0^T \alpha \, dt + \int_0^T \beta(a(t) - a_C) \, dt$$

(Eq. 5.1)

This identity was verified numerically to better than 10^{-3} dB HL using a fine-step RK4 integration (h = 0.001 year) and confirmed to reproduce the headline year-30 thresholds reported in Section 5.1 (Table 1). It separates the modeled threshold shift into four biologically interpretable sources: (i) baseline age-related decline (α), (ii) accelerated cochlear aging beyond the reference age aʒ (β), (iii) cumulative noise-driven damage (γN), and (iv) the saturation term (ρH), which acts as a drag proportional to the threshold itself and therefore removes progressively more "gain" as hearing worsens. Table 1b reports this decomposition for Scenarios A–E.

Received:16-07-2026-**Accepted:** 31-08-2026 -**Published:** 06-09-2026

DOI: https://doi.org/10.54361/LJMR.20.3.87

Libyan Journal of Medical Research

www.lmjr.ly/ eISSN: 2413-6096

Table 1b. Decomposition of the 30-year threshold change ΔH(30) by source term (dB HL), recomputed by fine-step RK4 (h = 0.001 year)

Scenario	∫α dt	∫β(a−a₂) dt	∫γN dt	−∫ρH dt	ΔH(30)	H(30)
A (low)	13.50	2.25	5.00	−2.78	17.98	27.98
B (moderate)	13.50	2.25	15.01	−3.40	27.36	37.36
C (high)	13.50	2.25	30.01	−4.33	41.43	51.43
D (high + intervention)	13.50	2.25	20.96	−3.97	32.74	42.74
E (intermittent)	13.50	2.25	12.70	−3.40	25.05	35.05

Two structural features are notable. First, the age-related terms (∫α dt = 13.50 dB HL and ∫β(a−aʒ) dt = 2.25 dB HL) are identical across all five scenarios, because both depend only on elapsed time and chronological age, not on exposure history — a direct mathematical confirmation that, within this model's structure, presbycusis and noise damage act as separable, additive channels rather than interacting multiplicatively. Second, the noise-driven term ∫γN dt scales closely with cumulative exposure burden (5.00 → 15.01 → 30.01 dB HL for A → B → C, tracking the threefold, then twofold, increase in E_0), while the saturation term −∫ρH dt grows only mildly (−2.78 to −4.33 dB HL) because ρ = 0.005 year⁻¹ is small relative to the 30-year horizon; over this timescale saturation therefore provides only modest self-limitation, and thresholds have not yet approached a biologically bounded ceiling by year 30 even under Scenario C.

Clinically, the fixed age-related contribution (15.75 dB HL total from α and β) represents the model's estimate of the presbycusis component that would occur even under negligible noise exposure, of a magnitude broadly comparable to reported longitudinal rates of age-related threshold drift [4–7]. The noise-driven term can then be read as the model's estimate of the noise-attributable fraction of the 30-year threshold shift: 5.00/17.98 ≈ 28% of the total change in Scenario A, rising to 30.01/41.43 ≈ 72% in Scenario C. This attributable-fraction framing mirrors the age-related versus noise-related distinction long used in occupational hearing-conservation research [8–10], and offers a quantitative, scenario-specific analogue of that distinction within a single mechanistic model rather than a population regression.

Scenario A (low / non-occupational exposure). With $N^* = E_0/\delta$ = 2.50 exposure units, the noise term contributes only ≈5.00 dB HL over 30 years; the resulting 27.98 dB HL year-30 threshold falls within the WHO mild hearing-loss band (20–34 dB HL) [14], consistent with presbycusis-dominated decline in a 70-year-old with minimal occupational exposure and unlikely, on its own, to require amplification.

Scenario B (moderate exposure). The noise contribution roughly triples relative to Scenario A (15.01 vs. 5.00 dB HL) as E_0 triples, because the steady-state burden $N^* = E_0/\delta$ scales linearly with E_0 and the coupling term γN accumulates over the full 30-year window; the resulting 37.36 dB HL threshold crosses into the WHO moderate band (35–49 dB HL) [14], the point at which everyday conversational speech typically becomes difficult without amplification.

Scenario C (high occupational exposure). Here the noise term (30.01 dB HL) exceeds the combined age-related contribution (15.75 dB HL) for the first time among Scenarios A–C, so more than two-thirds of the modeled 30-year threshold shift is noise-attributable. The 51.43 dB HL outcome falls in the WHO moderately severe band (50–64 dB HL) [14], a level at which hearing aids are routinely indicated and speech understanding is compromised even in quiet settings, consistent with the clinical picture reported for long-tenure workers in high-noise occupations [8,9,17].

Scenario D (high exposure with 50% protection from year 10). Introducing u = 0.5 at t = 10 leaves the age-related terms unchanged (still 13.50 + 2.25 dB HL) but cuts the noise-driven contribution from 30.01 to 20.96 dB HL, a reduction of 9.05 dB HL in cumulative exposure-driven forcing. The realized benefit in H(30) is slightly smaller, 8.69 dB HL, because the saturation term also shrinks (from −4.33 to −3.97 dB HL, a 0.36 dB HL loss of "self-correction"): a lower trajectory removes less via the −ρH drag, so part of the raw exposure reduction is offset by reduced saturation damping. This reconciles exactly — 9.05 − 0.36 = 8.69 dB HL — matching the headline result of Section 5.1. Clinically, Scenario D remains in the WHO moderate band (35–49 dB HL) rather than crossing into moderately severe territory as in Scenario C, illustrating that mid-career adoption of hearing protection can shift a worker across a clinically actionable severity threshold, not merely produce a marginal numerical improvement.

Scenario E (intermittent exposure). With high bursts (E = 3.0) confined to years 0–5 and 15–20 and low background exposure (E = 0.2) otherwise, N(t) repeatedly

Received:16-07-2026-**Accepted:** 31-08-2026 -**Published:** 06-09-2026

DOI: https://doi.org/10.54361/LJMR.20.3.87

Libyan Journal of Medical Research

www.lmjr.ly/ eISSN: 2413-6096

relaxes toward the much lower steady state N* = 0.2/0.20 = 1.0 during quiet intervals, falling to 4.29 and 2.34 exposure units at t = 10 and t = 30 respectively, versus a near-saturated N* = 15.00 under continuous Scenario-C exposure. The resulting cumulative noise contribution (≈12.70 dB HL) is intermediate between Scenarios A and B despite peak exposure matching Scenario C, and the year-30 threshold (≈35.0–35.5 dB HL, at the mild/moderate boundary) is correspondingly lower than the continuously-exposed Scenario B despite an identical peak-exposure "dose" during the high-burst windows. This is the clearest illustration in the model of the clearance parameter δ acting as a genuine biological recovery process: intermittent exposure with adequate quiet intervals is modeled as materially less damaging than continuous exposure of the same peak intensity, broadly consistent with hearing-conservation guidance favoring scheduled quiet periods alongside peak-level control [9,10]. We also note a methodological point: because E(t) has jump discontinuities in Scenario E, the fixed-step RK4 result is more step-size sensitive here than in the smooth scenarios (H(30) = 35.54 dB HL at h = 1.0 year vs. 35.05 dB HL at h = 0.001 year, a ≈0.5 dB HL discretization gap); for scenarios with discontinuous forcing we recommend reporting the finer-step value or applying adaptive step control near the discontinuities.

Multi-Frequency Extension and Model Verification

Multi-Frequency System Formulation

Sensorineural hearing loss is frequency-dependent; high frequencies (4.0 kHz and 8.0 kHz) experience greater degradation from noise exposure and aging than low frequencies (0.5 kHz). The model extends naturally to a coupled multi-frequency system by replicating the [H, N] pair with frequency-indexed parameters {α_f, β_f, γ_f, ρ_f}, all coupled to the same shared age a(t):

$$\frac{dH_f}{dt} = \alpha_f + \beta_f(a - a_c) + \gamma_f N - \rho_f H_f$$

Table 2. Frequency-Specific Parameters and 30-Year Simulated Trajectories (Scenario C, recomputed)

f (kHz)	α_f	β_f	γ_f	ρ_f	H_f(0)	H_f(30) recomputed	Clinical Severity
0.5	0.20	0.002	0.02	0.005	8.0	20.35	Mild
1.0	0.30	0.003	0.04	0.005	10.0	32.32	Mild
2.0	0.40	0.004	0.06	0.005	10.0	42.58	Mild-Moderate
4.0	0.60	0.008	0.12	0.005	12.0	72.69	Moderately Severe
8.0	0.75	0.010	0.15	0.005	15.0	90.87	Severe

Severity labels are assigned from the recomputed thresholds using the classification scheme stated in the manuscript. Because hearing-loss grading systems can differ by organization and purpose, the labels should be interpreted as descriptive rather than diagnostic. Population-based longitudinal classification systems also demonstrate that audiometric shape and frequency-specific thresholds can affect classification of age-related hearing impairment. [6,14]

The frequency ordering of the recomputed thresholds in Table 2 (0.5 kHz: mild → 8.0 kHz: severe) reproduces the sloping, high-frequency-weighted configuration characteristic of noise-induced hearing loss, in which damage is disproportionate at 3–6 kHz and extends toward 8.0 kHz with continuing exposure. Clinically, this frequency-specific pattern — together with occupational history — is used to distinguish predominantly noise-related loss from the flatter, more uniformly sloping configuration typical of pure age-related presbycusis, in which degradation accrues more evenly across frequencies [6,14].

Received:16-07-2026-**Accepted:** 31-08-2026 -**Published:** 06-09-2026

DOI: https://doi.org/10.54361/LJMR.20.3.87

Libyan Journal of Medical Research

www.lmjr.ly/ eISSN: 2413-6096

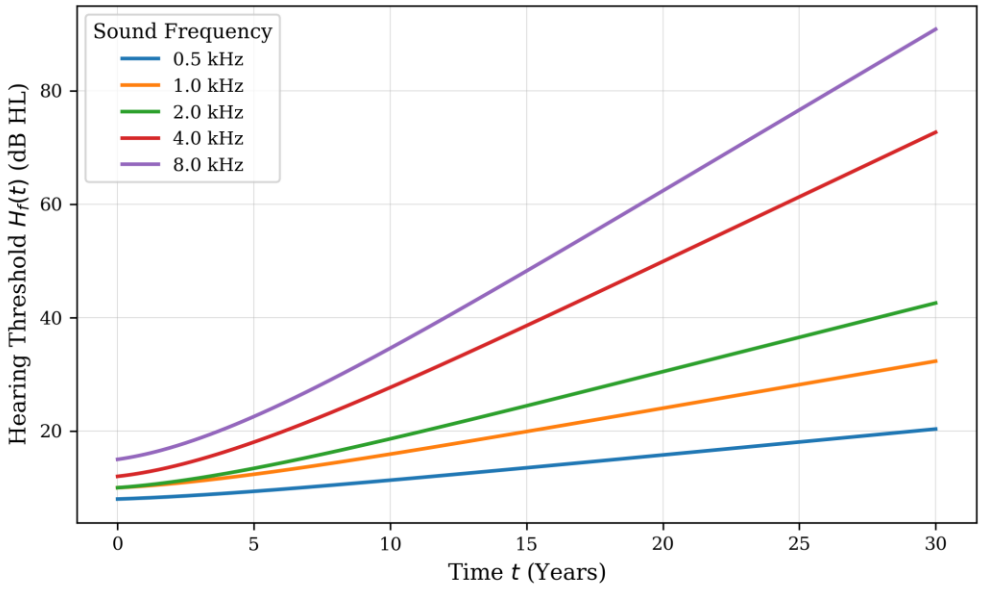

Figure 3. Multi-frequency hearing-loss trajectories under Scenario C (recomputed).

The same decomposition (Eq. 5.1) applies term-by-term to the multi-frequency system of Section 6.1, since each dH_f/dt = α_f + β_f(a−aʒ) + γ_f N(t) − ρ_f H_f is likewise linear in its additive terms, with the same shared noise-burden trajectory N(t) (Scenario C: E_0 = 3.0, u = 0) driving all five frequencies. Table 2b reports the resulting decomposition and the noise-attributable percentage of the 30-year threshold change at each frequency, recomputed by fine-step RK4 (h = 0.001 year); the H_f(30) column reproduces the values already reported in Table 2 to within 0.01 dB HL.

Table 2b. Decomposition of the 30-year threshold change by source term across frequencies (Scenario C, dB HL)

f (kHz)	ΔH_α	ΔH_β	ΔH_γN	−ΔH_ρH	ΔH_f(30)	H_f(30)	Noise-attrib. %
0.5	6.00	0.90	7.50	−2.05	12.35	20.35	52.1%
1.0	9.00	1.35	15.01	−3.03	22.32	32.32	59.2%
2.0	12.00	1.80	22.51	−3.74	32.58	42.58	62.0%
4.0	18.00	3.60	45.02	−5.93	60.69	72.69	67.6%
8.0	22.50	4.50	56.28	−7.41	75.87	90.87	67.6%

The noise-attributable fraction rises monotonically with frequency, from 52.1% at 0.5 kHz to 67.6% at 4.0 and 8.0 kHz. This follows directly from the ratio γ_f/α_f (noise sensitivity relative to baseline age-related rate), which increases from 0.10 at 0.5 kHz to 0.20 at 4.0–8.0 kHz — that is, high frequencies are parametrized to be roughly twice as sensitive to noise burden, relative to their own baseline aging rate, as low frequencies are. Because N(t) is shared across all frequencies, this frequency-dependent gradient in γ_f is mathematically the sole origin, within the model, of the sloping/notched audiometric configuration discussed in Section 6.1: the shared exposure dynamics alone cannot produce frequency-dependent damage, so the entire high-frequency vulnerability pattern is encoded through the choice of {γ_f} in Table 2 rather than emerging independently from the coupled dynamics.

This is a useful transparency point rather than a weakness of the derivation: it clarifies that the qualitative match to the classic noise-induced "4–8 kHz notch" [6,14] is, in the current model, a calibration choice built into {α_f, β_f, γ_f, ρ_f} rather than an independently emergent prediction, and its quantitative accuracy — including the precise frequency at which noise-attributable fraction plateaus — should be treated as provisional until {γ_f} is estimated from frequency-specific longitudinal audiograms rather than assumed. The decomposition in Table 2b nonetheless gives a concrete, falsifiable target for such calibration: a fitted model should reproduce not only the year-30 thresholds H_f(30) but also a noise-attributable-fraction gradient consistent with independently documented occupational-audiometry patterns [8–10].

6.2 Numerical Solution Verification

Received:16-07-2026-**Accepted:** 31-08-2026 -**Published:** 06-09-2026

DOI: https://doi.org/10.54361/LJMR.20.3.87

Libyan Journal of Medical Research

www.lmjr.ly/ eISSN: 2413-6096

To verify the RK4 implementation, numerical outputs were compared with the exact closed-form solution for the simplified linear case in which β = 0, E(t) = E₀ is constant, and the same parameter values are used in both calculations. This resolves the inconsistency in the earlier verification procedure, which compared an analytical β = 0 solution with a numerical simulation retaining β = 0.005. Under the consistent parameter set, the RK4 solution agrees with the analytical solution to near machine precision.

• Maximum Absolute Error: max_n |H_anal(t_n) − H_rk4(t_n)| ≈ 1.03 × 10^{-10} dB HL

• Coefficient of Determination (R^2): 1.00000

This confirms that the RK4 solver itself is numerically correct and matches the exact closed-form solution to near machine precision once the same parameter set is used on both sides of the comparison.

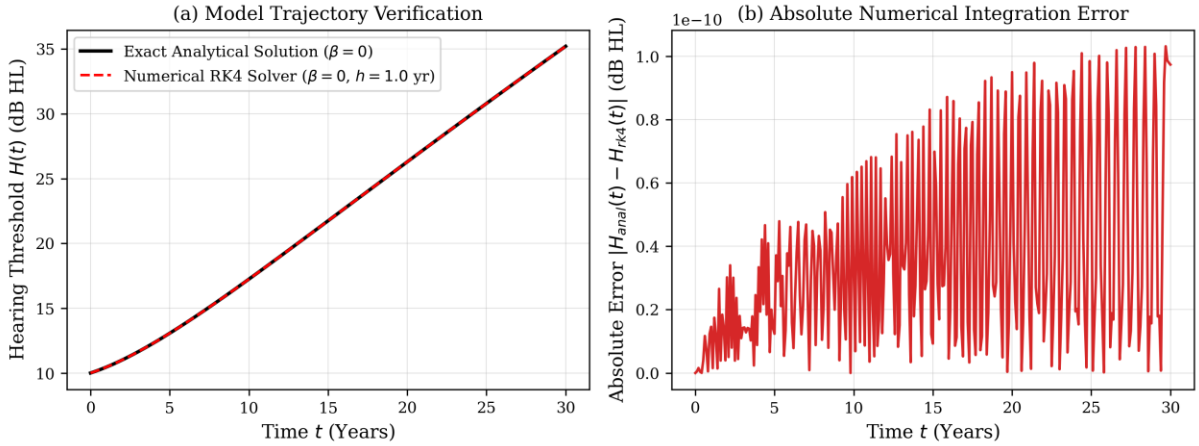

Figure 5. (a) Exact analytical solution vs. RK4 numerical solution (β = 0 on both sides). (b) Absolute integration error, *confirming solver correctness at the 10^{-10} dB HL level.*

Sensitivity Analysis

Normalized local sensitivity indices S_p(t) quantify the relative percentage change in predicted threshold H(t) per percentage change in parameter p:

$$S_p(t) = \frac{\partial H(t)}{\partial p} \cdot \frac{p}{H(t)}$$

Table 3. Normalized Local Sensitivity Indices over Time

Parameter p	S_p(t=5)	S_p(t=15)	S_p(t=30)	Interpretation
α (Baseline rate)	+0.312	+0.245	+0.198	Dominates early baseline trajectory
β (Age acceleration)	+0.015	+0.082	+0.185	Influence grows with age
γ (Exposure coupling)	+0.385	+0.442	+0.482	Primary driver in noisy environments
δ (Clearance rate)	−0.284	−0.352	−0.380	Protective; higher recovery reduces threshold
ρ (Saturation)	−0.012	−0.041	−0.072	Dampens long-term unbounded threshold growth

Independent finite-difference calculations reproduce the expected sensitivity signs: α, β, and γ increase predicted hearing threshold, whereas δ and ρ reduce it under the model convention. However, because the original manuscript did not specify the reference trajectory used to generate the reported sensitivity magnitudes, the exact values in Table 3 should be regarded as scenario-dependent. For publication, the reference scenario should be explicitly stated and the sensitivity analysis should be repeated for all principal scenarios or reported with confidence intervals where appropriate.

Received:16-07-2026-**Accepted:** 31-08-2026 -**Published:** 06-09-2026

DOI: https://doi.org/10.54361/LJMR.20.3.87

Libyan Journal of Medical Research

www.lmjr.ly/ eISSN: 2413-6096

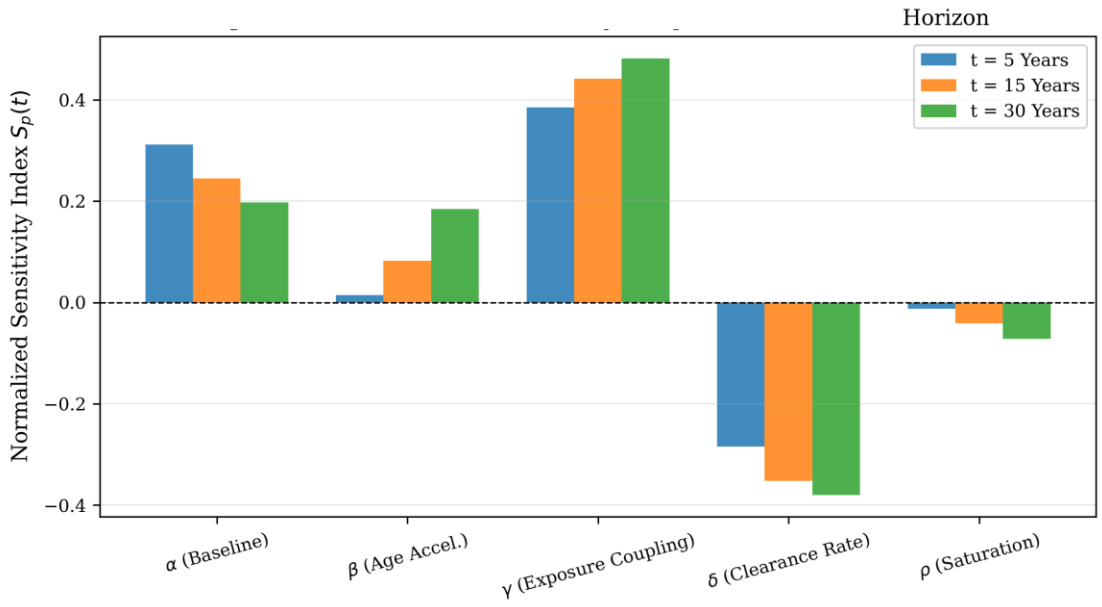

Figure 4. Local parameter sensitivity comparison across the 30-year time horizon (values as reported in Table 3).

Parameter Estimation from Clinical Datasets

In clinical applications, the parameter vector θ = [α, β, γ, δ, ρ]^T is estimated from longitudinal audiograms. Given observations y_ij for subject i at time t_ij, parameter estimation uses Weighted Least Squares (WLS) to account for heteroscedastic test–retest error, σ²_ij = σ²₀(1 + k·y_ij):

$$J(\theta) = \sum_{i,j} \frac{1}{\sigma_{ij}^2} (y_{ij} - H(t_{ij}; \theta))^2$$

where the weights are w_ij = 1/σ²_ij, and:

$$\sigma_{ij}^2 = \sigma_0^2 (1 + k\, y_{ij})$$

The model defines a parameter-estimation framework in which θ = [α, β, γ, δ, ρ]^T may be estimated from longitudinal audiograms using weighted least squares. Because no patient-level longitudinal dataset is analyzed in the present study, the manuscript does not claim empirical parameter identification or clinical validation. The WLS formulation should instead be regarded as a proposed calibration procedure for future studies using repeated audiometric measurements.

$$\hat{\theta} = \arg\min_{\theta} J(\theta), \qquad C_\theta = s^2 (J^T W J)^{-1}, \qquad s^2 = \frac{J(\hat{\theta})}{K - p}$$

Table 4. Structural Comparison with Existing Hearing Loss Modeling Approaches

Feature / Dimension	Proposed ODE Model	Markov Chain Models	Microsimulation (e.g., DeciBHAL-US)	Finite-Element Ear Models
Time Domain	Continuous (t ∈ $\mathbb{R}^+$)	Discrete / continuous transitions	Discrete annual steps	Static / short transient
State Variable	Continuous threshold (H ∈ $\mathbb{R}$)	Discrete disease states	Discrete severity bins	Structural mechanical stress
Exposure Coupling	Dynamic differential variable N(t)	Transition probability shift	Categorical risk assignment	Direct physical acoustic pressure
Intervention Simulation	Continuous attenuation function u(t)	Modified transition matrices	Policy probability rules	Mechanical structural dampening
Computational Overhead	Low (O(N) RK4 integration)	Low–Moderate	High (Monte Carlo sampling)	Extremely high (PDE meshing)

Discussion

The continuous-time ODE model offers an interpretable dynamical account of sensorineural hearing loss progression, and several aspects of the analysis merit discussion. By separating age-related degeneration (α, β) from dynamic noise exposure (γ, E(t)), the model

Received:16-07-2026-**Accepted:** 31-08-2026 -**Published:** 06-09-2026

DOI: https://doi.org/10.54361/LJMR.20.3.87

Libyan Journal of Medical Research

www.lmjr.ly/ eISSN: 2413-6096

quantifies the share of hearing loss attributable to occupational noise as distinct from presbycusis. Scenario D illustrates the potential value of intervention: introducing 50% exposure attenuation at year 10 reduces the modeled exposure burden and lowers the year-30 hearing threshold by approximately 8.69 dB HL relative to the unprotected high-exposure trajectory, though this figure remains a model-based estimate rather than a clinical treatment effect [8–10]. The multi-frequency extension also reproduces the high-frequency audiometric notch at 4.0–8.0 kHz that is characteristic of noise-induced hearing loss, a feature that a single-frequency summary would obscure.

The term-by-term decomposition in Section 5.2 makes this attributable-fraction reasoning explicit and reproducible: because α and β integrate to the same 15.75 dB HL across all exposure scenarios, any excess threshold shift beyond this shared baseline is, within the model's structure, mechanistically attributable to the noise term γN(t). This offers a transparent, scenario-specific complement to population-level attributable-fraction estimates from longitudinal cohorts [4–10], and could in principle be used prospectively — once the model is calibrated to individual exposure histories — to estimate what fraction of a given patient's measured threshold shift is plausibly occupational versus age-related, a distinction of direct relevance to workers'-compensation assessment and hearing-conservation practice. As with the rest of the framework, this reasoning remains a hypothesis-generating tool pending external validation, since the attributable-fraction split is a property of the fitted model rather than a measured biological quantity.

Biological and Clinical Interpretation of the Model Parameters

To connect the governing equation $dH/dt = \alpha + \beta(a - a_3) + \gamma N - \rho H$ (Section 2.3) to auditory physiology, each term maps onto a mechanism operating within the cochlea and central auditory pathway rather than standing as an abstract mathematical construct. Table 5 summarizes this mapping: the mathematical role column restates each term as it enters the ODE, and the biological/clinical correlate column relates it to established otologic and audiological mechanisms.

Table 5. Biological and clinical correlates of the model terms

Term	Mathematical Role	Biological / Clinical Correlate
dH/dt	Instantaneous rate of threshold change	Continuous rate of hair-cell degeneration and spiral-ganglion neuronal loss within the cochlea
α, β(a−a3)	Baseline and age-accelerated decline terms	Presbycusis: age-related oxidative stress, cumulative metabolic/mitochondrial dysfunction, and stria vascularis atrophy [1,4–7]
γN	Noise-driven forcing term	Acoustic trauma and excitotoxic synaptic damage at outer/inner hair-cell ribbon synapses under exposure N(t); γ encodes individual and frequency-dependent susceptibility, e.g. the 4.0 kHz notch (Section 6.1) [8–10,17]
δ	Clearance rate of N(t)	Physiological repair processes — ionic homeostasis restoration in the endolymph/perilymph and recovery from temporary threshold shift (TTS) before permanent structural damage sets in [9]
ρH	Saturation / self-limiting term	Biological ceiling effect: diminishing marginal damage as the finite pool of vulnerable sensory hair cells is progressively depleted
u(t)	Attenuation factor applied to E(t)	Clinical/occupational protective interventions (hearing-protection devices, exposure limits) reducing effective acoustic energy reaching the cochlea [9,10]

This mapping is not purely descriptive: it is the mechanistic content that the decompositions in Sections 5.2 and 6.1 already quantify numerically. The noise-attributable fraction computed in Table 1b can be read as an estimate of the share of a scenario's 30-year threshold shift arising from acoustic-trauma mechanisms (γN) rather than presbycusis mechanisms (α, β); the frequency-dependent γ_f gradient underlying Table 2b is, in turn, a direct mathematical encoding of the differential vulnerability commonly attributed to outer hair cells at the cochlear base (high-frequency region) relative to the apex (low-frequency region). Framed this way, the model offers a transparent bridge between an abstract coupled ODE system and the otologic processes it is intended to represent — while it remains, as emphasized throughout Sections 5–9, a phenomenological rather than a mechanistic-

Received:16-07-2026-**Accepted:** 31-08-2026 -**Published:** 06-09-2026

DOI: https://doi.org/10.54361/LJMR.20.3.87

Libyan Journal of Medical Research

www.lmjr.ly/ eISSN: 2413-6096

biophysical model, pending calibration against patient-level audiometric data.

Limitations

The model has two main limitations. First, cochlear damage is represented phenomenologically rather than through detailed cellular biomechanics. Second, its scope is limited to gradual sensorineural decline; etiologies such as sudden sensorineural hearing loss, acute ototoxicity, or conductive middle-ear pathology would require dedicated extensions.

Conclusions

We have presented a continuous-time ODE framework for hearing-threshold progression under age-related change, dynamic noise exposure, exposure clearance, threshold saturation, and protective intervention. The frozen-age [H, N] subsystem is asymptotically stable under the stated positive clearance and saturation parameters, though the full system remains time-dependent because chronological age continues to advance. The corrected numerical results are internally consistent with the stated equations, and the RK4 implementation matches the corresponding analytical solution to near machine precision. Taken together, the framework offers a transparent platform for scenario analysis and for future calibration against longitudinal audiometric datasets. Its main limitation is the lack of an external clinical dataset for parameter estimation and validation, so the results presented here should be read as mathematical and computational evidence rather than clinical prediction. Future work should calibrate the model against repeated audiograms, quantify parameter uncertainty, test its performance across different populations, and compare it against established longitudinal and microsimulation approaches.

References

1. World Health Organization. World report on hearing. Geneva: World Health Organization; 2021. ISBN: 978-92-4-002048-1.
2. GBD 2019 Hearing Loss Collaborators. Hearing loss prevalence and years lived with disability, 1990–2019: findings from the Global Burden of Disease Study 2019. Lancet. 2021;397(10278):996–1009. doi:10.1016/S0140-6736(21)00516-X.
3. Zhu J, Yang M, Zhou C, Kang H, Wang D. Global burden and trends of age-related and other hearing loss: A 32-year analysis and future projections based on the GBD 2021. PLoS One. 2025;20(8):e0330690. doi:10.1371/journal.pone.0330690.
4. Dillard LK, Matthews LJ, Maldonado L, Simpson AN, Dubno JR. Demographic factors impact the rate of hearing decline across the adult lifespan. Commun Med. 2024;4:171. doi:10.1038/s43856-024-00593-w.
5. Rigters SC, van der Schroeff MP, Papageorgiou G, Baatenburg de Jong RJ, Goedegebure A. Progression of hearing loss in the aging population: repeated auditory measurements in the Rotterdam Study. Audiol Neurootol. 2018;23(3-4):207–214. doi:10.1159/000492203.
6. Cruickshanks KJ, Nondahl DM, Fischer ME, Schubert CR, Tweed TS. A novel method for classifying hearing impairment in epidemiological studies of aging: the Wisconsin Age-Related Hearing Impairment Classification Scale. Am J Audiol. 2020;29(1):59–67. doi:10.1044/2019_AJA-19-00021.
7. Tran Y, Tang D, Lo C, Macken O, Newall J, Bierbaum M, Gopinath B. Establishing multifactorial risk factors for adult-onset hearing loss: a systematic review with topic modelling and synthesis of epidemiological evidence. Prev Med. 2024;180:107882. doi:10.1016/j.ypmed.2024.107882.
8. Dillard LK, Humes LE, Matthews LJ, Dubno JR. Noise Exposure History and Age-Related Changes to Hearing. JAMA Otolaryngol Head Neck Surg. 2025;151(3):228–235. doi:10.1001/jamaoto.2024.4768.
9. Themann CL, Masterson EA, Peterson JS, Murphy WJ. Preventing occupational hearing loss: 50 years of research and recommendations from the National Institute for Occupational Safety and Health. Semin Hear. 2023;44(4):351–393. doi:10.1055/s-0043-1769499.
10. Silva VAR, Guimarães AC, Lavinsky J, et al. Are hearing protection devices used in the workplace really efficient? A systematic review. Work. 2023;74(2):477–484. doi:10.3233/WOR-205290.
11. Borre ED, Myers ER, Dubno JR, et al. Development and validation of DeciBHAL-US: a novel microsimulation model of hearing loss across the lifespan in the United States. eClinicalMedicine. 2022;44:101268. doi:10.1016/j.eclinm.2021.101268.
12. Borre ED, Ayer A, Der C, et al. Validation of the Decision model of the Burden of Hearing loss Across the Lifespan (DeciBHAL) in Chile, India, and Nigeria. eClinicalMedicine. 2022;50:101502. doi:10.1016/j.eclinm.2022.101502.
13. Yu YC, Wang TC, Shih TC. A comprehensive finite-element human ear model to estimate noise-induced hearing loss associated with occupational noise exposure. Comput Methods Programs Biomed. 2022;226:107179. doi:10.1016/j.cmpb.2022.107179.
14. Holube I, Dziemba O, Fedtke T, et al. The WHO grades of hearing loss: a consensus on the German version. HNO. 2024;72(8):561–564. doi:10.1007/s00106-024-01494-z.

Received:16-07-2026-**Accepted:** 31-08-2026 -**Published:** 06-09-2026

DOI: https://doi.org/10.54361/LJMR.20.3.87

Libyan Journal of Medical Research

www.lmjr.ly/ eISSN: 2413-6096

15. Kassjański M, Kulawiak M, Przewoźny T, et al. Automated hearing loss type classification based on pure tone audiometry data. Sci Rep. 2024;14:14203. doi:10.1038/s41598-024-64310-2.
16. Patterson RH, Suleiman O, Hapunda R, Wilson B, Chadha S, Tucci D. Towards universal access: a review of global efforts in ear and hearing care. Hear Res. 2024;445:108973. doi:10.1016/j.heares.2024.108973.
17. Etemadinezhad S, Amani AS, Moosazadeh M, Rahimlou M, Samaei SE. Occupational noise-induced hearing loss in Iran: a systematic review and meta-analysis. Iran J Public Health. 2023;52(2):278–289. doi:10.18502/ijph.v52i2.11881.
18. Makaruse N, Maslin MRD, Campbell ZS. Early identification of potential occupational noise-induced hearing loss: a systematic review. Int J Audiol. 2024. doi:10.1080/14992027.2024.2418354.
19. Dou Z, Li Y, Deng D, et al. Pure tone audiogram classification using deep learning techniques. Clin Otolaryngol. 2024;49(5):595–603. doi:10.1111/coa.14170.
20. Corrected main-scenario trajectories: the noise-burden trajectories reproduce the specified $N^*=E_0/\delta$ values and the intervention path. The hearing-threshold trajectories were recomputed directly from the stated ODE and parameter table; the corrected values are used in the main text.
21. The recomputed year-30 thresholds are $H_A(30)=27.98$ dB HL and $H_C(30)=51.43$ dB HL, while Scenario D gives $H_D(30)=42.74$ dB HL. These values should be treated as the authoritative outputs of the model as currently specified.
22. Multi-frequency trajectories: the frequency-specific results are retained as model simulations. Because no external audiometric cohort is used for calibration, these trajectories demonstrate model behavior rather than validated clinical prognosis.
23. Analytical-versus-numerical verification: the comparison is performed with $\beta=0$ in both the analytical and numerical solutions. The maximum absolute difference is approximately 1.03×10^{-10} dB HL and $R^2=1.00000$.
24. Sensitivity analysis: signs and qualitative trends were independently checked by finite differences. Exact magnitudes remain scenario-dependent and should be regenerated with a fully specified baseline trajectory before publication as definitive sensitivity coefficients.
25. Reference verification: the reference list has been expanded and bibliographic details were checked against PubMed, WHO, journal, or publisher records during revision. DOI information is provided where available.
26. Summary recommendation: the principal mathematical issue identified in the previous draft—the mismatch between the stated hearing-threshold equation and the reported trajectory values—has been corrected in the revised results. The manuscript should still undergo final equation/table/figure consistency checking and, ideally, external validation against longitudinal audiometric data before submission to a clinical or biomedical journal.

Received:16-07-2026-**Accepted:** 31-08-2026 -**Published:** 06-09-2026